Atmospheric
Chemistry
and Physics

Open Access

Reactive oxygen species associated with water-soluble PM$_{2.5}$ in the southeastern United States: spatiotemporal trends and source apportionment

V. Verma[1], T. Fang[1], H. Guo[1], L. King[1], J. T. Bates[1], R. E. Peltier[2], E. Edgerton[3], A. G. Russell[1], and R. J. Weber[1]

[1]Georgia Institute of Technology, 311 Ferst Drive, Atlanta, GA 30328, USA
[2]University of Massachusetts Amherst, 686 North Pleasant Street, Amherst, MA 01003, USA
[3]Atmospheric Research & Analysis, 410 Midenhall Way, Cary, NC 27513, USA

Correspondence to: R. J. Weber (rodney.weber@eas.gatech.edu)

Abstract. We assess the potential of the water-soluble fraction of atmospheric fine aerosols in the southeastern United States to generate reactive oxygen species (ROS) and identify major ROS-associated emission sources. ROS-generation potential of particles was quantified by the dithiothreitol (DTT) assay and involved analysis of fine particulate matter (PM) extracted from high-volume quartz filters (23 h integrated samples) collected at various sites in different environmental settings in the southeast, including three urban-Atlanta sites, in addition to a rural site. Paired sampling was conducted with one fixed site in Atlanta (Jefferson Street), representative of the urban environment, with the others rotating among different sites, for ∼ 250 days between June 2012 and September 2013 ($N = 483$). A simple linear regression between the DTT activity and aerosol chemical components revealed strong associations between PM ROS-generation potential and secondary organic aerosol (WSOC – water-soluble organic carbon) in summer, and biomass burning markers in winter. Redox-active metals were also somewhat correlated with the DTT activity, but mostly at urban and roadside sites. Positive matrix factorization (PMF) was applied to apportion the relative contribution of various sources to the ROS-generation potential of water-soluble PM$_{2.5}$ in urban Atlanta. PMF showed that vehicular emissions contribute uniformly throughout the year (12–25 %), while secondary oxidation processes dominated the DTT activity in summer (46 %) and biomass burning in winter (47 %). Road dust was significant only during drier periods (∼ 12 % in summer and fall). Source apportionment by

chemical mass balance (CMB) was reasonably consistent with PMF, but with higher contribution from vehicular emissions (32 %). Given the spatially large data set of PM sampled over an extended period, the study reconciles the results from previous work that showed only region- or season-specific aerosol components or sources contributing to PM ROS activity, possibly due to smaller sample sizes. The ubiquitous nature of the major sources of PM-associated ROS suggests widespread population exposures to aerosol components that have the ability to catalyze the production of oxidants in vivo.

1 Introduction

Substantial research has been dedicated to understanding the mechanisms by which ambient particulate matter (PM) causes adverse health effects in humans (Hoek et al., 2002; Samet et al., 2000; Gauderman et al., 2007; Stayner et al., 1998; Riediker et al., 2004; Sun et al., 1984; Sagai et al., 1993; Donaldson et al., 1996, 1997, 2003; Li et al., 2003, 2009a; Delfino et al., 2013). In many of these studies, a large number of PM health effects have been attributed to the oxidative or oxidant generating properties of ambient particles (Donaldson et al., 1996, 2003; Li et al., 2003, 2009a; Delfino et al., 2013). It has been hypothesized that several oxidative mechanisms can arise simultaneously, leading to a cascade of events that results in high concentrations of reactive oxygen species (ROS) in vivo (Tao et al., 2003; Castro and Free-

man, 2001; Donaldson et al., 2003). ROS concentrations in excess of the antioxidant capacity to neutralize them leads to oxidizing other cellular components, which eventually translates into numerous health outcomes (Delfino et al., 2005; Li et al., 2009a; Peters et al., 2006).

Based on this possible mechanistic route linking aerosol chemistry to health, numerous studies have been initiated in the past several years focused on measuring the oxidative properties of ambient particles. A variety of probes have been developed to quantify different aspects of PM-induced oxidative stress. These include chemical systems that mimic the loss of antioxidants, such as oxidation of dithiothreitol (DTT assay; Cho et al., 2005), glutathione (GSH; Godri et al., 2011), ascorbic acid (AA; DiStefano et al., 2009; Mudway et al., 2004), covalent bonding with glyceraldehyde-3-phosphate dehydrogenase (GAPDH; Rodrigueza et al., 2005), and hydroxyl radical generation in the presence of H$_2$O$_2$ (Shi et al., 2003). Other probes measure cellular responses when exposed to aerosols; such as macrophage ROS generation (Landreman et al., 2008), the induction of heme oxygenase-1 (HO-1) and other stress protein expressions (Li et al., 2003), and cytokine activation (Wilson et al., 2010). Each of these assays represents a plausible mode of PM toxicity and collectively they should be considered as the toolkit for deconstructing the complex mechanisms of PM ROS generation. One advantage of these assays, is that they are integrative of various aerosol chemical properties, and as pointed out by several researchers (Ayres et al., 2008; Venkatachari and Hopke, 2008; Kuenzli et al., 2004), many of them can serve as a screening step for assessing the PM samples/emission scenarios for more detailed chemical analysis and downstream health studies.

The DTT assay was devised to simulate the in vivo generation of superoxide radicals, wherein DTT was used as a surrogate of the biological reducing agents (NADH and NADPH) (Kumagai et al., 1997, 2002). When incubated at 37 °C with a test PM sample, a decreasing DTT concentration over time is inferred as a measure of the ROS-generating capability of the particles. A number of pure chemicals have been found to be associated with the response of this assay, e.g., quinones have been known to catalyze the transfer of electrons from DTT to oxygen (Kumagai et al., 2002). In a recent study, certain transition metals (e.g., Fe, Cu and Mn) have also been shown to be active in this assay (Charrier and Anastasio, 2012). However, evidence showing that any of these chemicals play a substantial role in the DTT activity of ambient PM in a range of environments (locations) is limited. The major components of the ambient PM identified so far to be associated with the DTT activity are often bulk groups of species such as organic carbon (OC), both water-soluble (WSOC) and insoluble (WIOC) and water-soluble HULIS (humic-like-substance) compounds (a class of WSOC characterized by strong hydrophobicity). However, most of these associations have been inferred based on statistical correlations (Ntziachristos et al., 2007; Verma et al., 2009a, b; Hu et

al., 2008; Biswas et al., 2009b), which do not necessarily establish causation, while very few have used semimechanistic approaches such as physical separation of the organic compounds and metals (Verma et al., 2011; Lin and Yu, 2011; Charrier and Anastasio, 2012).

Both approaches have merits; however, a major concern with the studies solely based on regression analysis of DTT activity vs. chemical components is related to the sample size (N); most are based on $N < 30$ with very few exceeding 100 (e.g., Delfino et. al., 2013; $N = 111$), which limits the statistical significance of the inferred associations. This is partly due to analytical complexity of the DTT assay, which entails a laborious and time intensive protocol. To address this problem, we developed a semiautomated instrument involving minimal manual operation. The instrument, which has been described in detail in Fang et al. (2014), allowed us to conduct the DTT assay on a large number of aqueous samples (~ 1200) as part of the Southeastern Center for Air Pollution and Epidemiology (SCAPE) study.

SCAPE is a collaborative center – combining five multidisciplinary studies from Georgia Tech and Emory University – aimed at achieving a better understanding of the ambient PM health effects. Along with describing the automated DTT analytical method in our previous paper from the center's studies, Fang et al. (2014) showed that the DTT activity of ambient fine aerosols collected from various sites and seasons in the southeastern US is generally correlated with PM mass; however, the strength and slope of the correlation varied ($R^2 = 0.40 - 0.90$; slope $= 0.01 - 0.05$ nmol min^{-1} µg^{-1}) among different sites and seasons. Here we discuss the detailed spatial and temporal profiles of the PM ROS-generation potential measured by the DTT assay on these samples. The bulk and specific chemical components, i.e., OC, elemental carbon (EC), WSOC, inorganic ions, water-soluble brown carbon (BrnC), and various water-soluble transition metals, were also measured. Both univariate linear regression and receptor modeling techniques were used to identify and apportion the contribution of major emission sources to the ROS-generating potential of ambient particles in the southeastern US. This analysis focuses only on the water-soluble extracts from filter samples, while other reports will present results involving water-insoluble components and isolated chemical fractions of both water-soluble and insoluble species. The paper presents a unique and possibly the largest data set on PM ROS-generation potential (N, the number of filter samples $= 483$), linked to a range of aerosol sources that varies over seasons of the year, and thus provides a broader regional view of fine particle ROS characteristics.

Table 1. Sampling plan and details of sampling dates at each site.

Season, year	Sapling dates		Sampling site			
	Start date	End date	Fixed site	Samples collected (N)	Mobile site	Samples collected (N)
Summer, 2012	8 Jun 2012	20 Jul 2012	JST	31	YRK	33
	24 Jul 2012	31 Aug 2012	JST	37	GT	38
Fall, 2012	6 Sep 2012	4 Oct 2012	JST	26	RS	29
Winter, 2012–2013	15 Nov 2012	30 Nov 2012	JST	13	JST	14
	6 Dec 2012	4 Jan 2013	JST	22	YRK	22
	27 Jan 2013	27 Feb 2013	JST	30	RS	31
	5 Mar 2013	27 Mar 2013	JST	23	GT	22
Summer, 2013	**16 Jun 2013**	**16 Jul 2013**	**CTR**	**31**	**BHM**	**31**
Fall, 2013	9 Sep 2013	3 Oct 2013	GT	25	RS	25
Total number of samples				238		245

Note: In the summer of 2013 (shown in bold) measurements were made at sites outside of the State of Georgia as part of other studies to provide a greater context and were not part of the paired sampling approach with JST as the central site.

2 Experimental methods

2.1 Sampling plan

The sampling plan for SCAPE involved paired simultaneous measurements using two instrumented sites, one of which was fixed at the Jefferson Street SEARCH (Southeastern Aerosol Research and Characterization) site (Edgerton et al., 2005, 2006; Hansen et al., 2003), the other was rotated among three satellite sites, i.e., Yorkville, Roadside Atlanta, and Georgia Tech, all in Georgia. The sampling covered the period from June, 2012 to September, 2013; details of the sampling dates at each site are provided in Table 1. Each paired deployment lasted roughly 1 month, and was repeated in different seasons. Based on the temperature profile in Atlanta during the sampling period, shown in Supplement Fig. S1, data are classified into 3 seasons – summer (June–August, 2012), fall (September, 2012 and 2013), and winter (November, 2012–March, 2013). To provide a broader perspective, additional measurements (summer, June–July 2013) were made in Alabama, at the SEARCH rural–urban pair: Centreville (rural) and Birmingham (urban).

2.2 Sampling sites

A map showing the locations of all sites is shown in Fig. 1. Jefferson Street is located roughly 4 km northwest of downtown Atlanta and is representative of urban Atlanta. The site is surrounded by commercial and residential buildings, with nearby street traffic patterns consistent with a mixed-use urban environment. The site has extensively been used in past studies characterizing urban-Atlanta air quality (Hansen et al., 2006; Marmur et al., 2005) and the data used in epidemiological studies (Sarnat et al., 2008; Strickland et al., 2010).

In this study, Jefferson Street is again used as representative of urban Atlanta, to which the other three satellite measurements (discussed next) are compared.

The Roadside site is located on the Georgia Tech campus adjacent (i.e., within a few meters) to the interstate highway I-75/85. The degree to which the site is under direct influence of emissions from approximately 280 000 vehicles per day on a 14-lane freeway depends on wind direction and wind speed. The traffic fleet is mostly (97 %) light-duty gasoline vehicles. Slow-moving traffic is typical during the morning and evening rush hour periods. Jefferson Street is located roughly 2 km from this highway.

The Georgia Tech site is situated between the Roadside and Jefferson Street sites on the Ford Environment Sciences and Technology building, top floor, ∼ 600 m from the interstate. This site is an intermediate location between the Roadside (direct freeway emissions) and urban background (Jefferson Street) that could moderately be impacted by the roadway emissions.

Yorkville, also a SEARCH site, is located in a rural environment approximately 70 km west of Atlanta, which is generally upwind. The site is surrounded by agricultural land (e.g., pastures) and forests, with the nearest residences at least 1 km away. There are no major roadways in the vicinity of the site and nearby traffic emissions are negligible.

As a contrast to Atlanta, measurements were also made in an additional southeastern US city. The urban Birmingham Alabama SEARCH site has several coking ovens within 10 km and a cast iron pipe foundry located approximately 400 m to the east. The site also receives emissions from nearby (< 4 km) freeways (I-65, US-31and I-20).

Centreville is the SEARCH rural pair site to Birmingham, located approximately 85 km south-southwest of Birming-
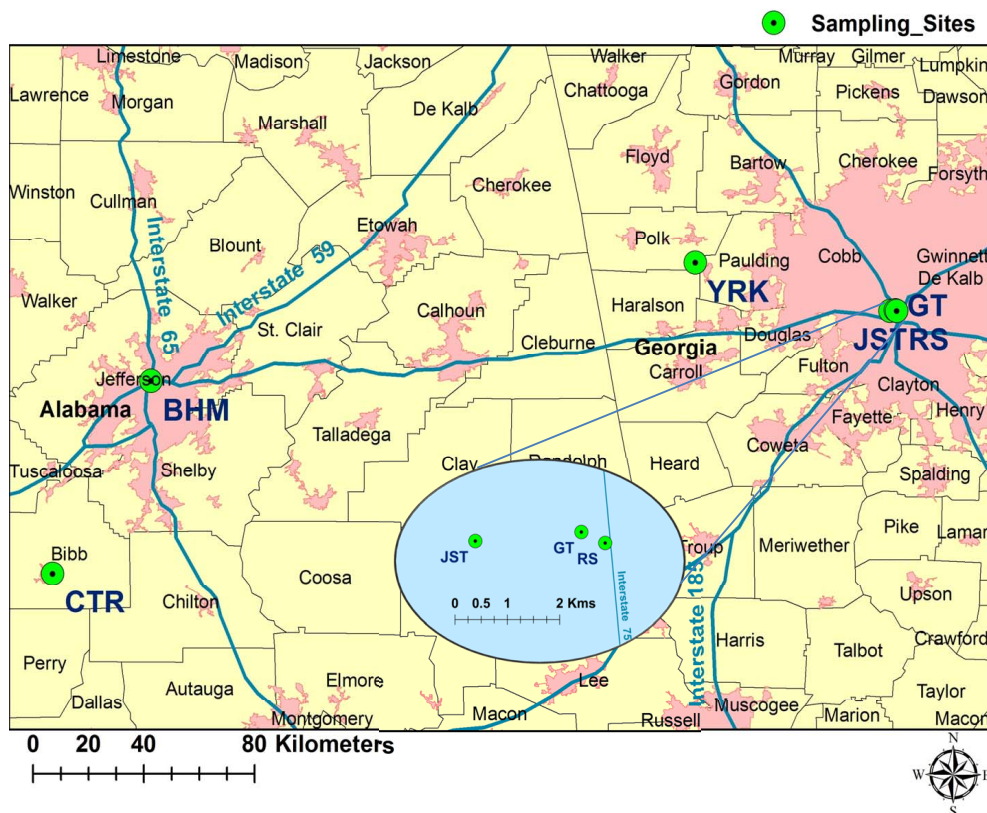
Figure 1. Map of sampling sites.

ham. The site is heavily wooded and is surrounded by the Talladega National Forest with a high density of oak and pine trees. Measurements were conducted simultaneously at Birmingham and Centreville and overlapped with the Southern Oxidant and Aerosol Study (SOAS).

Detailed descriptions of all of the SEARCH sites used in this study can be found elsewhere (Hansen et al., 2003). The Jefferson Street, Roadside, Georgia Tech, Yorkville, Birmingham and Centreville sites are referred to as JST, RS, GT, YRK, BHM and CTR respectively.

2.3 Filter collection and extraction protocol

A high-volume sampler (HiVol, Thermo Anderson, nondenuded, nominal flow rate 1.13 m^3 min^{-1}, PM$_{2.5}$ impactor) was set up at each site and fine particles were collected onto prebaked 8 × 10 in. quartz filters (Pallflex® Tissuquartz™, Pall Life Sciences). A total of 23 h of integrated samples (12:00–11:00) were collected daily during the sampling periods (Table 1) at each site, along with periodic field blanks (at least three per site per month). The number of samples collected from each site, approximately 30 per site per season (total = 483) is given in Table 1. After collection, the filters were wrapped in prebaked aluminum foil and immediately stored in a freezer (−18 °C). The chemical and ROS-generation analysis of the filters was started in March 2013.

Prior to the analysis, the filters were cut using a 1 in. diameter metallic punch. For the DTT activity, WSOC and BrnC analysis, three filter sections (1 in. diameter each) were extracted in 15 mL of deionized water (DI, Milli-Q; > 18 MΩ) via sonication in a water bath for 30 min, while additional punches were extracted separately in the same manner (15 mL of DI for 30 min of sonication time) for the metals (four punches) and inorganic ions (one punch) analysis. These extracts were then filtered using PTFE (polytetrafluoroethylene) 0.45 µm pore syringe filters (Fisherbrand). The filtered extracts for metals were acidified by adding nitric acid (high-purity trace metal grade; 2 % w/v final solution), consistent with current protocols (Henshaw et al., 1989; Talbot and Weiss, 1994).

2.4 Online instruments

PM$_{2.5}$ mass concentrations were monitored by a tapered element oscillating microbalance (TEOM, Thermo Scientific TEOM 1400a), operating continuously at JST, BHM, YRK and CTR throughout the sampling period (Atmospheric Research Analysis Inc. data). At other sites (RS and GT), summed concentrations from measured chemical components (EC + 1.6 OC + ions (SO$_4^{-2}$ + NH$_4^+$ + NO$_3^-$) + water-soluble metals), were used as a proxy for the PM mass concentrations. This method has been found to agree well with

the TEOM concentrations at JST and YRK sites, where co-located measurements were available (Fang et al., 2014).

2.5 Chemical analysis on PM filters

The WSOC and its light absorption properties (brown carbon, BrnC, used as a source tracer) were measured on HiVol extracts via an automated system using an autosampler (Dionex 40AS), spectrophotometer and total organic carbon (TOC) analyzer. BrnC was measured on an aliquot (300 µL) of the extracts via a liquid waveguide capillary cell (LWCC-2100, World Precision Instruments, Sarasota, FL), which was coupled to a UV–Vis spectrophotometer (USB4000 spectrometer, Ocean Optics, Dunedin, FL) (Hecobian et al., 2010). Following the waveguide, the aliquot was conducted to a Sievers TOC analyzer (Model 900, GE Analytical Instruments; Boulder, CO) for determination of WSOC concentration.

The automated system was also used to measure water-soluble metals, which involved nebulizing the water extracts and directing the aerosol stream to an XRF (X-ray fluorescence) instrument (Xact™ 625 Monitoring System), capable of online measurements of a range of elements. Details of the nebulizer-XRF system would be published in a subsequent publication. Briefly, 5 mL of the acidified PM water extracts was aerosolized using a continuous flow ultrasonic nebulizer (CETAC, U5000 AT$^+$). The resulting fine aerosol was conducted by a flow of clean filtered air through a drying system (a 136 °C heated section followed by a cooled section at −5 °C). The dried aerosol stream was neutralized by a Kr-85 source and mixed with clean filtered (Pall HEPA Capsule, part no. 12144) air to obtain the instrument sample flow rate of 16.7 L min^{-1}. A wide range of elements were measured by the instrument; however, we present only the relevant species which are either used as specific emission markers (Ca, dust (Coz et al., 2010), K, biomass burning (Artaxo et al., 1994)), or possibly play a role in ROS generation (Fe, Cu, Mn, Zn; Schoonen et al., 2006).

Elemental and organic carbon content of the PM was measured on a small section (1.45 cm^2) of the HiVol filters using a thermal/optical transmittance (TOT) analyzer (Sunset Laboratory) by the NIOSH (National Institute for Occupational Safety and Health) method (Birch and Cary, 1996). For the measurement of inorganic ions (SO$_4^{-2}$, NH$_4^+$, NO$_3^-$, etc.) at JST and GT, ion chromatography (IC) (LC30 chromatography oven, and Dionex CD20 conductivity detector, with IonPac® CS12A carboxylate-functionalized cation exchange and IonPac® AS12A carbonate eluent anion-exchange columns) was performed on the aerosol extracts of HiVol filters collected from those sites.

2.6 ROS-generation-potential measurement

ROS-generation potential of the ambient aerosols was measured by a semiautomated instrument (Fang et al., 2014) for measuring DTT activity of the PM extracts obtained from HiVol filters. The filters (about 18) for the DTT assay were extracted everyday and the extracts immediately returned to the freezer (−18 °C). Approximately two-thirds (∼ 12) of these extracts were kept for the DTT activity measurement overnight and the remaining one-third (∼ 6) were analyzed in the morning of the following day. The typical range of PM mass concentrations in the extracts used in the DTT assay was 10–25 µg mL^{-1}.

The semiautomated instrument is based on the protocol adopted from Cho et al. (2005) and uses two programmable syringe pumps (Kloehn, Inc., Las Vegas, NV, USA) for the mixing and transfer of reaction mixtures and reagents. The DTT oxidation in a mixture of DTT (1 mM; 0.5 mL), potassium phosphate buffer (0.5 M, pH = 7.4, Chelex treated; 1 mL) and PM extract (3.5 mL) is carried out in a single vial (conical centrifuge polypropylene tube), continuously shaken and maintained at 37 °C using a ThermoMixer (incubating accuracy: ±0.5 °C, Eppendorf North America, Inc., Hauppauge, NY, USA). A small aliquot (100 µL) of this reaction mixture is transferred to another vial at various time intervals (0, 4, 13, 23, 32 and 41 min) and mixed with trichloroacetic acid (TCA, 1 % w/v; 1 mL), Tris buffer (0.08 M with 4 mM EDTA; 2 mL) and 5,5′-dithiobis(2-nitrobenzoic acid) (DTNB; 0.2 mM; 0.5 mL). The final reaction mixture is pushed through a liquid waveguide capillary cell (LWCC-M-100; World Precision Instruments, Inc., FL, USA), coupled to an online spectrophotometer (Ocean Optics, Inc., Dunedin, FL, USA), to measure the absorption intensity at 412 nm. The rate of DTT consumption was calculated based on the linear regression slope of remaining DTT concentrations measured at various time intervals. The automated method provided a measurement of the DTT activity at a rate of 1 sample per hour. For each batch (consisting of either 7 or 14 samples), at least one field blank and one standard (9,10-phenanthraquinone, 0.095 µM; used as a positive control) were analyzed. Both blanks and standards were fairly consistent, with an average slope plus or minus the standard deviation of 0.38 ± 0.10 ($N = 45$) and 1.27 ± 0.19 ($N = 55$) µM min^{-1}, respectively. The automated system was cleaned periodically (generally after every 15 days, or unless the slope of the DTT reaction rate started to become nonlinear) by rinsing thoroughly with methanol (at least 3 times) followed by DI (at least 6 times). The whole DTT analysis was completed by January 2014. Given the long storage period of the filters in a freezer (varying from 6 to 12 months), the DTT activities measured on these samples represent the ROS-generation potential associated with only stable PM compounds.

2.7 Source apportionment analysis

The emission sources contributing to the ROS-generation potential of the particles were investigated using regression and receptor modeling techniques. As typically done in these

studies, a simple linear regression was conducted between the measured concentrations of various chemical components and DTT activity for each individual site and season. A rough indication of ROS sources was obtained based on the correlations between DTT activity and various species, and associating those species with sources. The large data set from the combined JST and GT sites, which are representative of urban-Atlanta air quality, allows for a more quantitative source apportionment. Two receptor models were used: positive matrix factorization (EPA-PMF, version 3.0) and chemical mass balance (EPA-CMB, version 8.2).

The detailed description and procedural details of PMF are described elsewhere (Paatero, 1997; Norris and Vedantham, 2008). The uncertainties for each chemical species used in PMF and CMB were the overall uncertainties obtained by propagating the uncertainties at each step starting from filter collection to analysis. The analytical uncertainties were obtained by analyzing the standards (e.g., 9,10-phenanthrenequinone for DTT, sucrose solution for OC and WSOC, copper sulfate for Cu, and ammonium iron (II) sulfate hexahydrate for Fe, etc.) or the same ambient sample (e.g., for BrnC) multiple times ($N > 6$) and calculating the standard deviation from the measurement. WSOC, BrnC, NH_4^+, SO_4^{-2}, and EC were classified as strong (high signal-to-noise ratio; S/N) species, while the metals K, Ca, Mn, Fe, Cu and Zn were categorized as weak (low S/N). DTT activity was chosen as the "total variable" and thus by default assigned as weak species. Missing values in the data were replaced by the species median. For the base runs ($N = 20$), a seed of 25 was chosen and the model was executed for factors 4, 5 and 6. The converged run with the highest goodness-of-fit parameter (lowest object function) was selected for five factors, which are identified as secondary WSOC, secondary SO_4^{-2}, vehicular emissions, road dust and biomass burning. With fewer factors, the individual tracer species started merging (e.g., dust and WSOC came in the same factor in a four-factor solution). For more than five factors, a converged solution was not obtained. The correlation among individual factors was tested by G-space plots. The solution space of these plots was filled by the contribution values indicating the independence of different factors.

In the CMB approach (Coulter, 2004), source contributions to PM$_{2.5}$ at JST were first determined and then the sources most associated with DTT activity were identified through correlations. The model was run using eight yearly average source profiles, which were derived from JST in a previous study (Marmur et al., 2005). Profiles included primary sources from gasoline vehicles (LDGV), diesel vehicles (HDDV), soil dust (SDUST), biomass burning (BURN), and coal fired power plants (CFPP). Secondary source profiles included ammonium sulfate (AMSULF), ammonium bisulfate (AMBSULF) and other OC (OTHROC), which is taken to be secondary OC (SOC). Using the JST–GT combined HiVol concentration data, which includes inorganic ions, water-soluble metals, OC and EC, contributions of each

source to the measured concentration of various species were predicted at JST on a daily basis. DTT activity was then related to these CMB-identified PM$_{2.5}$ source contributions through a stepwise regression analysis using the Akaike information criterion (AIC) approach (Akaike, 1974), with DTT activity as the dependent variable and sources' contributions as the independent variables. Note, the source profiles used total metals, whereas the fitting data were water-soluble metals; however, using total metals data from the SEARCH data archive for the sampling period showed little effect on the final DTT source apportionment. More detailed analysis based on the improved source profiles recently developed by an ensemble approach (Balachandran et al., 2014) is underway and here we only present the study's average results from the CMB to compare and validate the PMF analysis.

Data from the YRK, RS and Alabama sites (CTR and BHM) were not included in PMF and CMB as they represent more extreme and generally different conditions than JST and GT, the sites representative of urban Atlanta. These other sites also had insufficient data for their own source apportionment analyses.

3 Results and discussion

3.1 PM emission characteristics

3.1.1 Elemental, water-soluble organic and brown carbon (EC, WSOC, BrnC)

Figure 2a, b and c show the ambient concentrations of EC, WSOC and BrnC at all sites for different months of sampling. EC and WSOC are discussed first since they represent the diverse PM emission characteristics at these sites, followed by BrnC. EC is a marker for incomplete combustion, such as vehicular emissions (Schauer, 2003), while secondary oxidation processes (Weber et al., 2007) and biomass burning (Zhang et al., 2010) are the major sources of WSOC in the southeast. From these figures, contrasts can be made between paired sites, and seasonal trends can be discerned. Measurements in the Atlanta region can also be contrasted to the Alabama sites.

The monthly average concentrations of EC (Fig. 2a) are consistent with primary vehicular emissions being the dominant EC source; the concentrations are highly heterogeneous. Large concentration differences were observed for each pair, with highest EC at the RS site, followed by urban background sites (JST, GT, and BHM), and lowest concentrations at the rural sites (YRK and CTR). The JST–GT EC concentrations were similar, suggesting that GT is not highly influenced by the roadway emissions, and therefore more representative of EC levels in the metro area, similar to JST. The largest contrast in EC among paired measurements is between urban and rural sites. For both summer and winter seasons, EC is
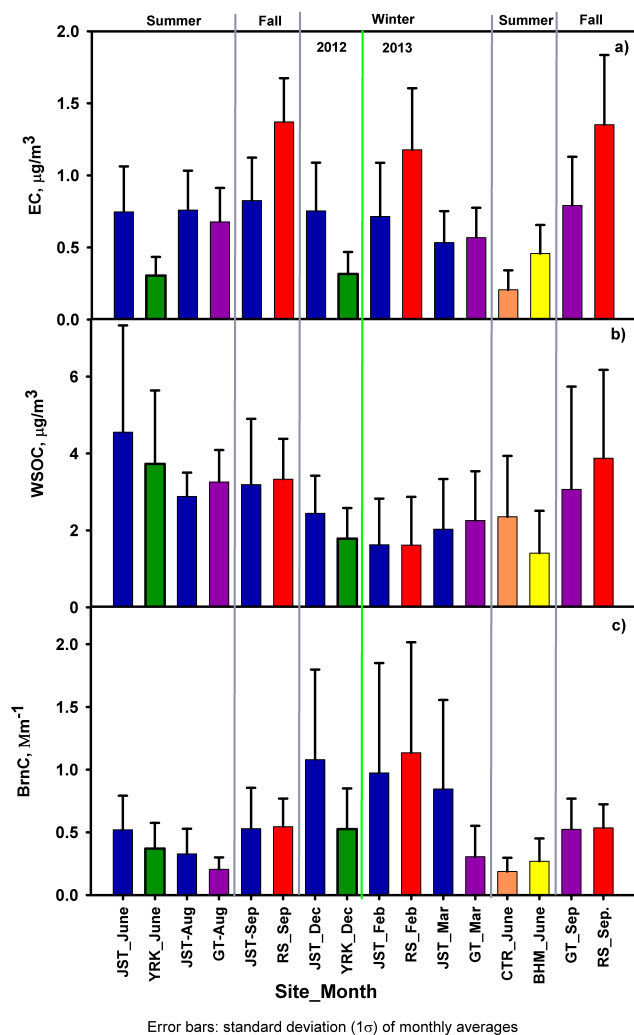
Figure 2. Monthly average ambient concentrations of EC **(a)**, WSOC **(b)**, and BrnC **(c)** at the sampling sites.

more than double at the urban sites (JST and BHM) compared to their respective rural component pair (YRK and CTR) (the mean plus or minus the standard deviation (1σ) of the ratio is 2.9 ± 1.6 in summer, and 2.7 ± 0.9 in winter for JST/YRK, and 2.92 ± 1.42 for BHM/CTR). The RS site has the highest concentration of EC in both fall and winter seasons (RS/JST = 1.81 ± 0.67 in fall, and 1.9 ± 0.8 in winter, and RS/GT = 1.95 ± 0.5 in fall).

There is little seasonal variation in the EC levels across most sites. For example, the average EC concentrations at JST in summer ($0.75 \pm 0.25 \, \mu g \, m^{-3}$), fall ($0.82 \pm 0.30 \, \mu g \, m^{-3}$), and winter ($0.67 \pm 0.33 \, \mu g \, m^{-3}$) were similar. The mean EC concentration at RS was slightly lower in winter ($1.18 \pm 0.43 \, \mu g \, m^{-3}$) than in fall ($1.37 \pm 0.30 \, \mu g \, m^{-3}$ in September, 2012, and $1.45 \pm 0.34 \, \mu g \, m^{-3}$ in September, 2013). The marginally lower levels of EC in winter seasons in Atlanta (JST, GT and RS sites) might be attributed to higher rainfall during these

periods (December–March; Fig. S1). Precipitation scavenging could have superseded the effect of generally reduced mixing height in winter on primary aerosol concentrations.

Unlike EC, WSOC was more spatially uniform, but varied substantially between different seasons (Fig. 2b). WSOC concentrations at the paired sites were very similar indicating that major WSOC sources extend to regional scales. These sources are mainly secondary organic aerosol (SOA) formation and biomass burning, (Zhang et al., 2010, 2012), with possibly minor influence from primary WSOC associated with vehicular emissions at the urban sites (Yan et al., 2009). An overall stronger influence of summertime SOA than wintertime biomass burning on WSOC in the region is apparent from a gradually decreasing averaged concentration profile at JST from summer to winter ($3.8 \pm 2.2 \, \mu g \, m^{-3}$, $3.2 \pm 1.7 \, \mu g \, m^{-3}$ and $2.0 \pm 1.1 \, \mu g \, m^{-3}$ in summer, fall and winter). Similar decreases are also noted at other sites (from $3.7 \pm 1.9 \, \mu g \, m^{-3}$ in summer to $1.8 \pm 0.8 \, \mu g \, m^{-3}$ in winter at YRK, and from $3.3 \pm 1.1 \, \mu g \, m^{-3}$ and $3.9 \pm 2.3 \, \mu g \, m^{-3}$ in fall, 2012 and 2013, respectively, to $1.6 \pm 1.3 \, \mu g \, m^{-3}$ in winter, 2013 at RS). These results are consistent with a more detailed analysis of the WSOC spatial and seasonal distribution conducted 2 years before in the southeastern US (Zhang et al., 2010).

BrnC denotes the water-soluble organic compounds that absorb light in the UV region of the UV–Vis spectrum (Hecobian et al., 2010). Biomass burning is by far the largest source of these compounds with additional contributions from vehicular sources and possibly aged SOA (Hecobian et al., 2010; Zhang et al., 2011). The spatial profile of BrnC (Fig. 2c) is intermediate between EC (heterogeneous) and WSOC (homogeneous), indicating the diversity of its sources. The moderate impact of vehicular emissions on BrnC is probably reflected in generally higher concentrations of BrnC at RS and other urban sites (JST, GT, BHM) than at rural sites (CTR, YRK). However, the strong seasonality is evident from its extreme values in winter periods resulting from biomass burning (average levels at JST in winter are $0.97 \pm 0.78 \, mM^{-1}$, compared to $0.42 \pm 0.25 \, mM^{-1}$ in summer and $0.53 \pm 0.33 \, mM^{-1}$ in fall).

3.1.2 Water-soluble metals

The selected elements (Fig. 3), have a wide range of concentrations at various sites and differing seasonal trends, pointing to heterogeneous sources. A more in-depth discussion on the distribution of the measured water-soluble elements will follow in a subsequent publication, here we only briefly discuss the major trends in selected metals. BHM, a site heavily impacted by industrial emissions, has very high concentrations of all metals, with Ca, Mn, and Zn the highest among all sites. After BHM, RS has the highest levels of most metals among all sites in the Atlanta region (i.e., JST, GT, YRK, RS), indicating either road dust and/or direct vehicular emissions as their major source. Rural sites, YRK and CTR, have
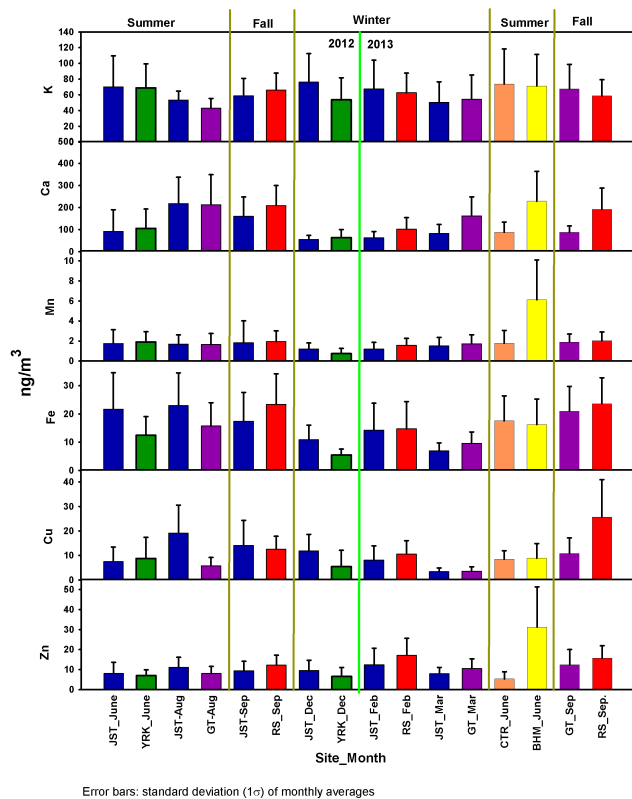
Figure 3. Monthly average ambient concentrations of water-soluble metals at the sampling sites.

Figure 4. Monthly averages of volume- (DTTv) and mass-normalized (DTTm) DTT activity at the sampling sites.

generally lower metal concentrations, while GT and JST levels are moderate.

Higher rainfall in winter compared to summer months could also affect the metal concentrations since the re-entrainment of road dust, which is a major source of metals, is most effective in dry periods. The metals of predominantly crustal and vehicular origin (e.g., Ca, Fe, Mn and Cu) are generally higher in summer and fall compared to the winter (Fig. 3). For example, the average Ca concentration at JST was 155 ± 116, 160 ± 87, and $67 \pm 37\,\mathrm{ng\,m^{-3}}$ in summer, fall, and winter, respectively. Exceptions are K and Zn, which despite being associated with crustal dust (K; Coz et al., 2010) or vehicular sources (Zn; Liu et al., 2008) are also emitted in biomass burning (Echalar et al., 1995), which could account for a weaker seasonal variability due to multiple sources; average K concentration is 62 ± 25, 59 ± 22 and $65 \pm 32\,\mathrm{ng\,m^{-3}}$ in summer, fall and winter, respectively, while the respective Zn concentration is 9.6 ± 4.7, 9.3 ± 4.8 and $9.9 \pm 5.8\,\mathrm{ng\,m^{-3}}$ at JST.

3.2 PM ROS-generation potential

Temporal and spatial differences in the water-soluble DTT activity are discussed to provide an overview of the PM ROS-generation potential in the southeastern US.
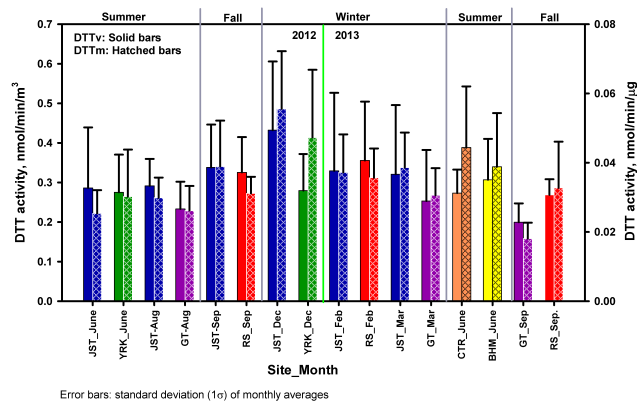
The time series of daily average DTT activity from the sites in different months is shown in our previous publication (Fang et al., 2014) and also reproduced in the Supplement (Fig. S2). The rate of DTT consumption is normalized by both the volume of sampled air (DTTv, expressed in units of $\mathrm{nmol\,min^{-1}\,m^{-3}}$; Fig. S2a) and the particulate mass (DTTm, expressed in units of $\mathrm{nmol\,min^{-1}\,\mu g^{-1}}$; Fig. S2b). A summary of the spatial and seasonal trends in mean DTT activity (both DTTv and DTTm) for the individual sampling periods and at various sites is shown in Fig. 4. Our measurements of both volume and mass normalized DTT activity are generally in the typical range (0.1–$1.5\,\mathrm{nmol\,min^{-1}\,\mu g^{-1}}$ for DTTv and 0.005–$0.1\,\mathrm{nmol\,min^{-1}\,\mu g^{-1}}$ for DTTm, as summarized in Fang et al., 2014) observed for ambient particles at other locations. Figure 4 shows that, in general, both the extrinsic (DTTv) and intrinsic (DTTm) activity of ambient PM is spatially uniform. There is no substantial difference in DTT activity of ambient PM at the two sites for any paired measurement, except the JST–YRK pair in winter (DTTv(YRK) < DTTv(JST)) and GT–RS pair in fall (DTTm(RS) > DTTm(GT)).

A significant seasonal variability in both the volume and mass normalized DTT activity is evident; the levels are generally higher in the colder months than in summer (Fig. 4). A one-sample t test showed that the DTTv at JST in December was significantly ($p \leq 0.05$) higher than those from June–July ($51 \pm 34\,\%$), August ($48 \pm 22\,\%$), and September ($27 \pm 14\,\%$). These results are in agreement with a recent study conducted in the Los Angeles Basin, which showed a generally higher DTT activity (both mass and volume normalized) of quasi-ultrafine particles in cooler months compared to warmer periods (Saffari et al., 2014). The authors in that study attributed the higher DTT activity to an elevated concentration of redox-active semivolatile organic compounds (SVOCs) caused by their enhanced partitioning to the particulate phase and the lowered atmospheric mixing height in winter. Although SVOCs have been suggested to
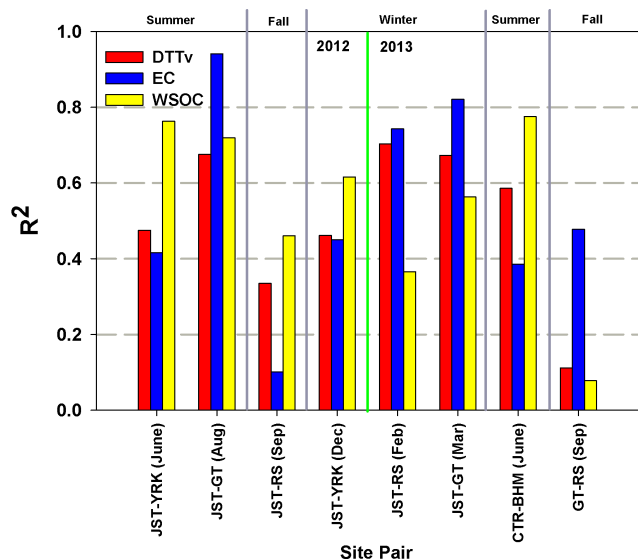
Figure 5. Site-to-site correlations (R^2) for volume normalized DTT activity (DTTv), EC and WSOC of PM$_{2.5}$.

make a substantial contribution to the DTT activity of ultrafine particles (Verma et al., 2011), the PM$_{2.5}$ samples collected via HiVol filters in our study are not expected to contain a significant fraction of these species due to losses associated with a large flow rate and long sampling duration (Ashbaugh and Eldred, 2004; Warner et al., 2001).

The seasonal variability is even more pronounced in the intrinsic DTT activity (Fig. 4). For example, differences in DTTm levels in December vs. June–July (119 ± 48 %), August (86 ± 31 %) and September (44 ± 14 %) are higher compared to the respective differences in DTTv levels. Similar increases in the intrinsic DTT activity in winter were observed at other sites too (38 ± 13 % at GT from average of August, 2012, and September, 2013, and 53 ± 24 % at YRK), but not at RS, where the average fall level (0.032 ± 0.009 nmol min^{-1} µg^{-1}) was nearly the same as in winter (0.036 ± 0.008 nmol min^{-1} µg^{-1}).

To further assess the spatiotemporal variability in DTTv activity in the region, correlation coefficients (R^2) were calculated for all of the site pairs and are shown in Fig. 5. To put the DTT activity comparison in a larger context, we have also included the corresponding coefficients for EC and WSOC. A high spatial correlation for a species indicates it has more spatially uniform emission sources in the region, on the scale of distances between the paired sites.

The site pair JST–GT shows high correlation coefficients ($R^2 > 0.5$) for many PM species (DTT, EC and WSOC), which was expected given their spatial proximity and absence of strong sources nearby, e.g., roadways. The other site pairs show disparate patterns for the different PM species depending upon their sources. For example, EC has relatively low correlation coefficients for the urban–rural site

pairs, i.e., JST–YRK in both summer ($R^2 = 0.42$) and winter (0.45), and BHM–CTR ($R^2 = 0.39$), as expected. Despite relatively close proximity, the low correlation in fall for the JST–RS pair ($R^2 = 0.10$) and the GT–RS pair ($R^2 = 0.48$) for EC is due to the strong influence of freeway emissions (I-85) at the RS site. However, the JST–RS correlation is high in February ($R^2 = 0.74$), possibly suggesting some contributions from a common source of EC, such as biomass burning.

WSOC however exhibits high correlations for most site pairs (JST–YRK, JST–GT, CTR–BHM; $R^2 > 0.5$) in all seasons (Fig. 5). The correlations are generally higher in summer ($R^2 > 0.70$), indicating a more regional influence of SOA formation as a source of WSOC in summertime, compared to biomass burning in winter ($R^2 < 0.65$). The correlations are generally weaker for the pairs involving RS ($R^2 = 0.08 - 0.46$), probably due to the added contribution of freeway emissions to WSOC.

Compared to WSOC and EC, the spatial correlations for DTT activity are moderate in all seasons. For example, R^2 for DTT is not as high as for EC for the sites in closer proximity ($R^2 = 0.68$ and 0.67 for JST–GT in fall and winter, respectively). Similarly, in summer, when the correlations for WSOC are very high even for the far-apart sites (JST–YRK and CTR–BHM), correlations for DTT are only moderate ($R^2 = 0.47$ and 0.59). It appears that DTT activity is impacted by both regional sources and local emissions associated with individual site characteristics. The role of various emission sources in the DTT activity of ambient PM in different seasons and sites is the major point of discussion in the next section and also the subsequent papers from this study.

3.3 Sources of PM ROS-generation potential

Sources of ROS-generation potential were identified and apportioned using a combination of linear regression, factor analysis and chemical mass balance techniques as described below.

3.3.1 Linear regression of DTT activity with PM chemical composition

Pearson's correlation coefficients for the linear regression between DTT activity and the measured chemical components were calculated for each site and season and are shown in Table 2. Considering the limited daily variability in mass normalized DTT activity at most sites in a given season (Fig. S2b), the regression was conducted on the volume normalized levels of DTT activity (nmol min^{-1} m^{-3}) and chemical components (µg m^{-3}). To consolidate the data for convenience, individual time series at JST and GT sites from June to August were merged (named "JST–GT summer"), given their similar concentration profiles. Similarly, JST and GT time series from December to March were merged as "JST–GT winter". The complete regression matrix showing

Table 2. Regression analysis (Pearson's R) between DTT activity and selected PM components.

Season	Site	WSOC	BrnC	Inorganic ions SO_4^{-2}	NH_4^+	OC	EC	Water-soluble metals K	Ca	Mn	Fe	Cu	Zn
Summer, 2012	JST–GT	**0.81**	**0.67**	**0.68**	**0.73**	**0.81**	**0.69**	0.49	0.20	**0.72**	**0.78**	**0.71**	0.62
	YRK	**0.79**	0.53	0.58	0.59	**0.76**	0.56	0.51	**0.68**	0.63	0.48	0.09	0.48
Fall, 2012	JST	**0.72**	**0.81**	0.49	0.52	**0.83**	**0.90**	0.61	−0.08	0.37	**0.74**	0.20	**0.82**
	RS	**0.71**	0.59	0.62	**0.66**	**0.77**	0.55	0.52	0.12	0.28	0.44	0.61	**0.68**
Winter, 2012–2013	JST–GT	**0.69**	**0.78**	0.15	0.13	**0.85**	**0.82**	**0.78**	−0.13	0.46	**0.65**	0.63	0.63
	YRK	**0.84**	**0.88**	0.34	0.45	**0.82**	**0.80**	**0.75**	0.31	**0.68**	0.04	0.43	**0.72**
	RS	**0.78**	**0.86**	0.47	0.52	**0.86**	**0.75**	**0.69**	0.31	0.49	0.57	0.35	0.60
Summer, 2013	CTR	**0.78**	**0.88**	**0.71**	**0.78**	**0.77**	**0.72**	**0.66**	0.23	0.36	0.41	−0.12	0.62
	BHM	**0.67**	**0.74**	**0.66**	**0.66**	**0.85**	**0.68**	0.41	0.55	**0.75**	**0.66**	0.23	**0.66**
Fall, 2013	GT	0.47	**0.75**	0.39	0.37	**0.79**	**0.78**	**0.65**	0.29	0.58	**0.66**	0.46	0.46
	RS	0.21	0.48	0.60	0.47	0.58	0.53	**0.74**	**0.79**	**0.84**	0.53	−0.09	**0.74**

Note: $R > 0.65$ are bold.

the correlation between all pairs of selected species, for each site and season, is provided in the Supplement (Table S1).

DTT activity is almost always correlated with OC in the present study. OC results from all major sources in the region (e.g., vehicular emissions, SOA, and biomass burning) and comprises the greatest fraction of PM mass (OM/PM$_{2.5} > 60\%$, not shown). Thus, the strong correlation of OC underlines the general contribution of PM organic compounds in the ROS-generation potential, and also likely accounts for the DTT correlation with PM mass, as reported in Fang et al. (2014). However, it does not yield any novel information on the specific PM species or the emission sources associated with the DTT activity. Associations between water-soluble DTT activity and organic compounds are consistent with a number of previous studies (Biswas et al., 2009a; Verma et al., 2012; Cho et al., 2005; Yang et al., 2014), but in contrast to other reports showing metals as the major drivers in this reaction (Charrier and Anastasio, 2012).

In summer, DTT activity is well correlated with WSOC at all sites; JST–GT ($R = 0.81$), YRK ($R = 0.79$), CTR ($R = 0.78$) and BHM ($R = 0.67$). Inorganic ions such as SO_4^{-2} and NH_4^+ are also correlated with WSOC and DTT activity ($R > 0.60$ at most sites) indicating secondary photochemical formation as their common source in summer. This is consistent with the results of ambient (Verma et al., 2009a) and chamber studies (McWhinney et al., 2013; Li et al., 2009b) suggesting higher DTT activity of secondary organic compounds than their parent gases and primary particles.

In addition to WSOC, summertime DTT activity at urban sites, i.e., JST–GT and BHM, is also correlated with certain transition metals (Mn ($R = 0.72$), Fe (0.78), and Cu (0.71) at JST–GT, and Mn (0.75), Fe (0.66) and Zn (0.66) at BHM). At BHM, the iron foundry and coke oven plants are the likely sources of these DTT-correlated metals. None of

these metals are strongly correlated with any specific emission markers at JST–GT. However, a moderate correlation of EC with DTT activity ($R = 0.69$) and also somewhat with metals ($R = 0.59$, 0.75 and 0.58 for Mn, Fe, and Cu; Table S1), suggests that vehicular emissions could be one of their common sources.

BrnC is also correlated with DTT activity in summer at the JST–GT, CTR, and BHM sites ($R > 0.65$). However, its correlation with both WSOC and EC ($R > 0.65$ at all sites; Table S1) does not allow isolating its predominant source. Both vehicular emissions and possibly aged SOA appear to contribute to these chromophores in summer.

In fall, DTT activity appears to be derived from a mixed contribution of primary vehicular emissions and secondary formation, as supported by its correlation with WSOC ($R = 0.72$), and EC ($R = 0.90$) at JST. Metals such as Fe and Zn are also correlated with DTT activity ($R = 0.70$ and 0.82) and EC ($R = 0.90$ and 0.75) at JST. The stronger correlation of primary emissions (EC) than secondary species (WSOC, SO_4^{-2}, NH_4^+) indicates a diminishing effect of photochemistry on the DTT activity. This is even more apparent in fall 2013, when the highest correlation of DTT at GT is with EC ($R = 0.78$), while the correlation with WSOC is low ($R = 0.47$).

However, at the RS site, road dust also appears to be a significantly contributing factor to DTT activity in fall as indicated from the moderate to strong correlation ($R = 0.61$–0.84) of certain metals including those from crustal sources (Cu and Zn in fall 2012, and K, Ca, Mn, and Zn in fall 2013). The added contribution from dust probably dilutes the association of DTT activity with other emission sources. For example, DTT at RS is not as strongly correlated with EC ($R \leq 0.55$) or WSOC ($R = 0.71$ and 0.21 in fall, 2012 and 2013, respectively) as at JST and GT.

In winter months, DTT activity is again correlated with WSOC at all sites; JST–GT ($R = 0.69$), YRK ($R = 0.84$), and RS ($R = 0.78$); however, this correlation is not accompanied by a similar correlation with inorganic ions ($R < 0.55$ for SO_4^{-2} and NH_4^+) as in summer months. This implies that another emission source of WSOC – biomass burning – starts contributing more to the DTT activity in winter. This is further reflected in the strong correlation of BrnC and K with DTT activity and WSOC ($R > 0.65$; Table 2 and Table S1) at all sites. In a study conducted in Los Angeles, the ambient concentrations of K and WSOC were elevated (~ 2 times) during the 2007 southern California wildfires compared to the postfire period (Verma et al., 2009b). More importantly, these wood-smoke particles were found to be at least 2 times more oxidative than the postfire ambient PM$_{2.5}$ typically dominated by vehicular emissions. The redox-active WSOC emitted in the biomass burning particles probably explains the higher intrinsic DTT activity of ambient PM in winter compared to other seasons in the present study (Fig. 4).

Interestingly, EC is also highly correlated with DTT activity ($R \geq 0.75$) in winter at all sites. However, the concurrent correlation of EC with BrnC and K ($R > 0.60$ at all sites; Table S1) somewhat confounds the contribution of vehicular sources with biomass burning to the DTT activity in winter. Although the EC / OC ratio for wood smoke can be very low (0.2–0.3; Harrison et al., 2012), it is possible that some fraction of EC at the sampling sites is also contributed by biomass burning in addition to the vehicular emissions. Transition metals are also correlated with DTT activity in winter months at JST–GT (Fe ($R = 0.65$), Cu ($R = 0.63$) and Zn ($R = 0.63$)), and YRK (Mn ($R = 0.68$), and Zn ($R = 0.72$)). However, the covariability of major emission markers in winter (i.e., EC, WSOC, K and BrnC) makes it difficult to identify their dominant source(s) at these sites.

3.3.2 Source contributions to DTT activity

To provide a more quantitative assessment of the contribution of various sources to the fine particle oxidative properties in urban Atlanta, a PMF analysis was conducted using the DTT activity and measured chemical composition data. The five factors resolved by PMF are shown in Fig. 6. Factors 1 and 2 are characterized with high WSOC and high inorganic ion (NH_4^+ and SO_4^{-2}) loadings, respectively. Both of these factors have higher relative contributions in summer and therefore are thought to be mostly associated with secondary oxidation processes; however, a significant EC fraction in factor 1 suggests some contribution of vehicular emissions to SOA. The lack of WSOC loading in secondary factor 2 is curious. Previous PM$_{2.5}$ source apportionment studies conducted in the southeastern US (Zhang et al., 2010, 2012) also showed a very low but nonzero WSOC fraction in this PMF factor. The results suggest that multiple mechanisms are involved in the formation of secondary WSOC and SO_4^{-2}. A more detailed analysis of the specific components of SOA for DTT activity
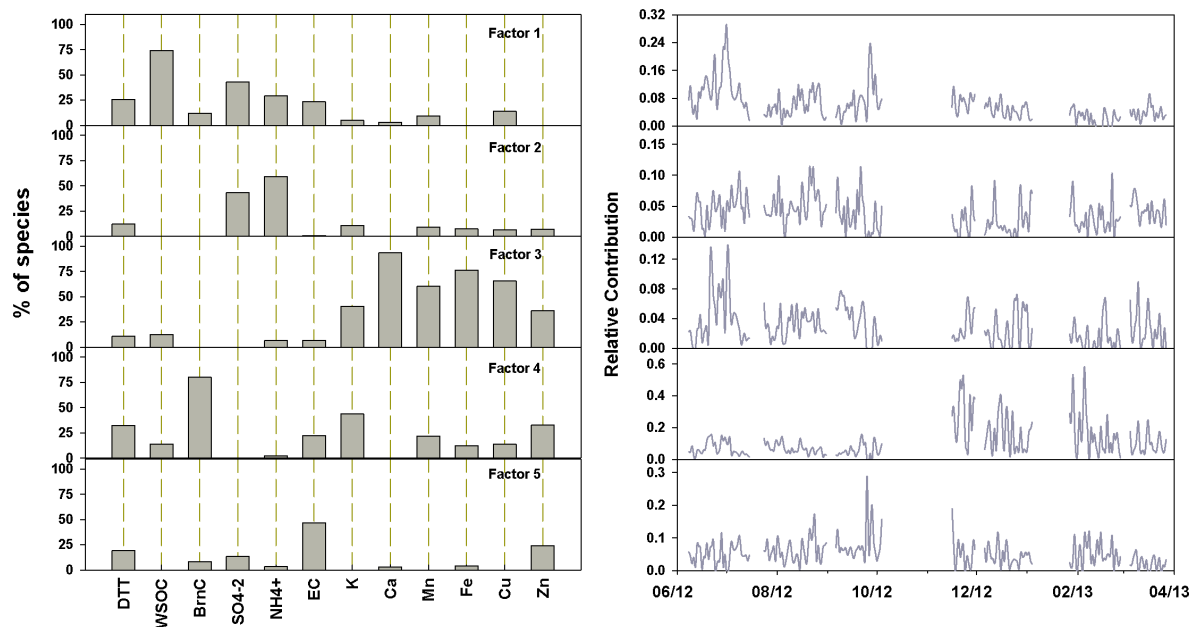
will be reported in the future. Here we assume that factor 2 is more representative of regional secondary aerosols, including some redox-active SOA, as there are no studies showing the DTT activity associated with the inorganic ions NH_4^+ and SO_4^{-2}.

Factor 3 has a very high loading of all metals and is attributed to road dust. This factor is also most significant in summer and fall, which is consistent with Fig. 3 showing a generally lowered concentration of metals in winter. Factor 4 has a clear signature of biomass burning with very high concentrations of BrnC and K, and is prominent in winter. Lastly, the EC peak in factor 5 is a distinct feature suggesting it is linked to primary vehicular emissions. Also consistent with the vehicular sources, this factor does not have an obvious seasonal pattern.

The time series of reconstituted DTT activity resolved by the five PMF factors, along with the residuals (not predicted) and a distribution of these factors in each season, is shown in Fig. 7. In summer, secondary oxidation processes (WSOC (29 %) + SO_4^{-2} (17 %), factors 1 and 2) are the dominant contributors (46 %) to DTT activity, with additional contributions from biomass burning (24 %, factor 4) and vehicle emissions (19 %, factor 5). In fall, the contribution from secondary formation drops to 32% (22 % associated with WSOC and only 10 % with SO_4^{-2} factors) with an increase in the contribution from vehicle emissions (25 %). Biomass burning dominates the ROS-generation potential in winter, contributing 47 % to the DTT activity, while relatively low contributions from secondary formation (20 %) and vehicle emissions (12 %) are observed. Road dust (factor 3) also makes a nonzero contribution to DTT activity, but is significant only in summer (13 %) and fall (11 %).

The seasonal contributions of various emission sources to DTT activity were averaged over the complete sampling year to estimate their aggregate contributions. Figure 8a shows that the major drivers of DTT activity of fine PM in Atlanta are biomass burning and secondary aerosols, with their respective annual contributions of 35 and 31 %. This is followed by vehicle emissions contributing 16 % annually, while road dust contributes minimally (9 %) to the DTT activity of PM$_{2.5}$. Together, all of these emission sources explained 91 % of the water-soluble DTT activity and 70 % of its variability (R^2 between reconstituted and measured DTT activity is 0.70; not shown) in Atlanta, demonstrating the robustness of our PMF model.

For the CMB analysis, step-wise regression provided a method for selecting the source contributions that significantly affect DTT activity, the others were removed from the regression to avoid overfitting. Thus, SDUST, CFPP and AMBSULF were removed from the regression through this

The scale for relative contribution of various factors (*y* axis on the right-side panel) has a different range for each factor.

Figure 6. Composition profiles (percentage of each species) for the five factors resolved by PMF (left panel), and the time series of their relative contribution (right panel).
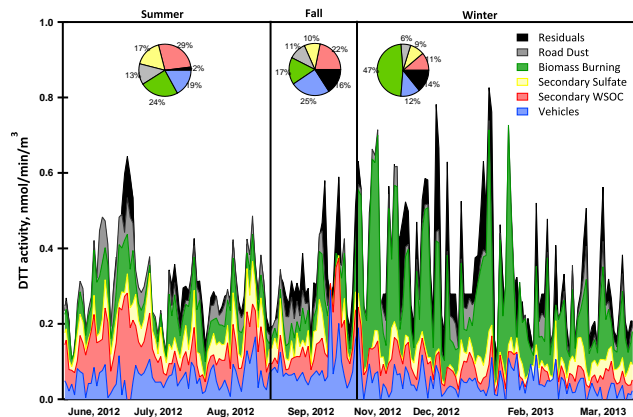

Figure 7. Time series of PM$_{2.5}$ DTT activity segregated into different factors as predicted by PMF and their seasonal contributions.

process. The final regression is

$$DTTv = 0.10\,LDGV + 0.072\,HDDV \quad (1)$$
$$+\,0.065\,BURN + 0.023\,AMSULF$$
$$+\,0.028\,SOC + 0.0069\,PMOther$$

PMOther, or the residual, was calculated as the difference between the measured PM$_{2.5}$ mass and the sum of the significant source contributions (i.e., LDGV, HDDV, BURN, AMSULF, SOC) for each day. All coefficients have *p* values of less than 0.01 except PMOther. The resulting Pearson's correlation coefficients (*R*) between DTTv and the various

sources were LDGV 0.60, HDDV 0.27, SDUST 0.15, BURN 0.49, CFPP 0.16, AMSULF 0.33, AMBSULF 0.03, and SOC 0.44.

The aggregate contribution of each of these sources to the PM$_{2.5}$ DTT activity over the whole study period is also shown in Fig. 8b. Overall, CMB yielded a similar picture as PMF; BURN and secondary oxidation processes (SOC + AMSULF) were the dominant sources of DTT activity in Atlanta with contributions of 33 and 29 %, respectively, in addition to vehicular sources (LDGV + HDDV, 32 %). CMB-identified vehicle sources also include road dust, which may explain, to some extent, a higher vehicular contribution to DTT activity by CMB compared to PMF.

4 Conclusions

Based on a large data set (*N* = 483), the ability of water-soluble PM$_{2.5}$ to generate oxidants determined by the DTT assay was linked with aerosol sources in the southeastern US. Spatial and temporal profiles of DTT activity in the region were produced from more than a year of sampling conducted intermittently at multiple sites, ranging from urban to rural environments. The PM chemical components indicated diverse emission characteristics at these sites in different seasons. While WSOC was spatially uniform from widespread summertime SOA formation and wintertime biomass burning emissions, primary pollutants such as EC and metals were less uniformly distributed and were higher at the ur-
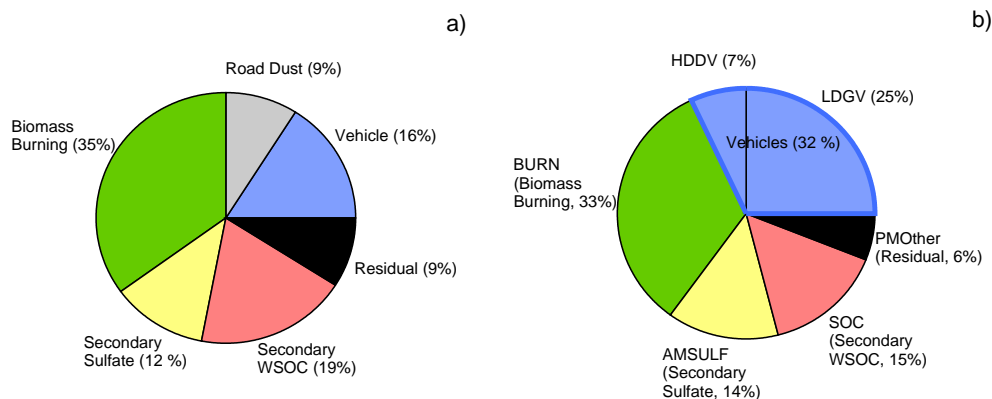
Figure 8. Annual aggregate contributions of different sources identified by PMF **(a)** and CMB method **(b)** to the water-soluble DTT activity of ambient PM$_{2.5}$ in urban Atlanta.

ban sites. The results show that DTT activity per volume of air sampled is also spatially uniform, but has seasonal variability with significantly higher levels in winter compared to summer and fall.

Despite the spatial uniformity, the moderate correlations of DTT activity between paired sites indicate the influence of both regional and local emissions on the PM's ability to generate ROS. A simple linear regression conducted between DTT activity and chemical components at each site in various seasons indicated that DTT activity is associated with WSOC in summer at both urban and rural sites, and probably influenced by vehicle emissions at urban sites. The associations of DTT activity with WSOC were moderate in fall, while those with vehicular emissions and road dust increased. In winter, DTT activity was best correlated with biomass burning (BrnC and K) at both urban and rural sites.

PMF analysis was conducted on the representative urban-Atlanta data set to quantify the contribution from each of these sources to the ROS-generating potential of PM. Biomass burning and secondary aerosol formation were quantified as the strongest sources of DTT activity, with their respective study-average (summer 2012–spring 2013) contribution of 35, and 31 %, followed by vehicular emissions (16 %). There was strong seasonality in the contribution from secondary and biomass burning aerosols, i.e., secondary processes dominated in summer accounting for 46 % of the DTT activity, while biomass burning in winter accounted for 47 %. The dust contribution was minimal (9 %) and was significant only in summer and fall. Source apportionment conducted using an alternative approach, CMB, also yielded similar study-average contributions from secondary sources (29 %) and biomass burning (33 %), but higher contributions from vehicular emissions (32 %), which is partly due to road dust included in the CMB-identified vehicular source.

This is perhaps the first study integrating an extensive data set on PM ROS-generating potential with chemical components using source apportionment models. It was made possible by a recently developed automated DTT analytical sys-

tem. Previous studies, relying on a small sample size collected from single sites and typically in a specific season have associated similar chemical species with aerosol DTT activity, but often from a limited range of sources. Further analysis is underway to resolve the specific components of SOA and biomass burning that contributed to the DTT activity. Finally, we note that the large spatial distribution of two major sources of DTT activity, secondary aerosols and biomass burning emissions, suggests a widespread exposure of populations to aerosol species capable of generating oxidants in vivo, and possibly leading to adverse health effects induced by oxidative stress.

The Supplement related to this article is available online at doi:10.5194/acp-14-12915-2014-supplement.

References

Akaike, H.: A New Look at the Statistical Model Identification, IEEE T. Automat. Contr., 19, 716–723, 1974.

Artaxo, P., Gerab, F., Yamasoe, M. A., and Martins, J. V.: Fine Mode Aerosol Composition at 3 Long-Term Atmospheric Monitoring Sites in the Amazon Basin, J. Geophys. Res.-Atmos., 99, 22857–22868, doi:10.1029/94jd01023, 1994.

Ashbaugh, L. L. and Eldred, R. A.: Loss of particle nitrate from Teflon sampling filters: Effects on measured gravimetric mass in California and in the IMPROVE network, J. Air Waste Manage., 54, 93–104, 2004.

Ayres, J. G., Borm, P., Cassee, F. R., Castranova, V., Donaldson, K., Ghio, A., Harrison, R. M., Hider, R., Kelly, F., Kooter, I. M., Marano, F., Maynard, R. L., Mudway, I., Nel, A., Sioutas, C., Smith, S., Baeza-Squiban, A., Cho, A., Duggan, S., and Froines, J.: Evaluating the toxicity of airborne particulate matter and nanoparticles by measuring oxidative stress potential – A workshop report and consensus statement, Inhal. Toxicol., 20, 75–99, doi:10.1080/08958370701665517, 2008.

Balachandran, S., Chang, H. H., Pachon, J. E., Holmes, H. A., Mulholland, J. A., and Russell, A. G.: Bayesian-based ensemble source apportionment of PM$_{2.5}$, Environ. Sci. Technol., 48, 2515–2515, doi:10.1021/Es500384y, 2014.

Birch, M. E. and Cary, R. A.: Elemental carbon-based method for monitoring occupational exposures to particulate diesel exhaust, Aerosol Sci. Tech., 25, 221–241, 1996.

Biswas, S., Verma, V., Schauer, J. J., Cassee, F. R., Cho, A. K., and Sioutas, C.: Oxidative potential of semi-volatile and non volatile particulate matter (PM) from heavy-duty vehicles retrofitted with emission control technologies, Environ. Sci. Technol., 43, 3905–3912, doi:10.1021/es9000592, 2009a.

Biswas, S., Verma, V., Schauer, J. J., Cassee, F. R., Cho, A. K., and Sioutas, C.: Oxidative potential of semi-volatile and non-volatile particulate matter (PM) from heavy-duty vehicles retrofitted with emission control technologies, Environ. Sci. Technol., 43, 3905–3912, 2009b.

Castro, L. and Freeman, B.: Reactive oxygen species in human health and disease, Nutrition, 17, 161–165, doi:10.1016/S0899-9007(00)00570-0, 2001.

Charrier, J. G. and Anastasio, C.: On dithiothreitol (DTT) as a measure of oxidative potential for ambient particles: evidence for the importance of soluble transition metals, Atmos. Chem. Phys., 12, 9321–9333, doi:10.5194/acp-12-9321-2012, 2012.

Cho, A. K., Sioutas, C., Miguel, A. H., Kumagai, Y., Schmitz, D. A., Singh, M., Eiguren-Fernandez, A., and Froines, J. R.: Redox activity of airborne particulate matter at different sites in the Los Angeles Basin, Environ. Res., 99, 40–47, 2005.

Coulter, C. T.: EPA-CMB8.2 Users Manual, Office of Air Quality Planning & Standards, US Environmental Protection Agency, Research Triangle Park, NC, 27711, 2004.

Coz, E., Casuccio, G., Lersch, T. L., Moreno, T., and Artinano, B.: Anthropogenic influenced mineral dust ambient fine particles at an urban site in Barcelona (Spain), Chem. Engineer. Trans., 22, 101–106, doi:10.3303/Cet1022016, 2010.

Delfino, R. J., Sioutas, C., and Shaista, M.: Potential role of ultrafine particles in associations between airborne particle mass and cardiovascular health, Environ. Health Persp., 113 934–946, 2005.

Delfino, R. J., Staimer, N., Tjoa, T., Gillen, D. L., Schauer, J. J., and Shafer, M. M.: Airway inflammation and oxidative potential of air pollutant particles in a pediatric asthma panel, J. Expo. Sci. Env. Epid., 23, 466–473, doi:10.1038/Jes.2013.25, 2013.

DiStefano, E., Eiguren-Fernandez, A., Delfino, R. J., Sioutas, C., Froines, J. R., and Cho, A. K.: Determination of metal-based hydroxyl radical generating capacity of ambient and diesel exhaust particles, Inhal. Toxicol., 21, 731–738, 2009.

Donaldson, K., Beswick, P. H., and Gilmour, P. S.: Free radical activity associated with the surface of particles: a unifying factor in determining biological activity?, Toxicol. Lett., 88, 293–298, 1996.

Donaldson, K., Brown, D. M., Mitchell, C., Dineva, M., Beswick, P. H., Gilmour, P., and MacNee, W.: Free radical activity of PM$_{10}$: iron-mediated generation of hydroxyl radicals, Environ. Health Persp., 105, 1285–1289, 1997.

Donaldson, K., Stone, V., Borm, P. J. A., Jimenez, L. A., Gilmour, P. S., Schins, R. P. F., Knaapen, A. M., Rahman, I., Faux, S. P., Brown, D. M., and MacNee, W.: Oxidative stress and calcium signaling in the adverse effects of environmental particles (PM$_{10}$), Free Radical Bio. Med., 34, 1369–1382, 2003.

Echalar, F., Gaudichet, A., Cachier, H., and Artaxo, P.: Aerosol emissions by tropical forest and savanna biomass burning – characteristic trace-elements and fluxes, Geophys. Res. Lett., 22, 3039–3042, doi:10.1029/95gl03170, 1995.

Edgerton, E. S., Hartsell, B. E., Saylor, R. D., Jansen, J. J., Hansen, D. A., and Hidy, G. M.: The southeastern aerosol research and characterization study: Part II. Filter-based measurements of fine and coarse particulate matter mass and composition, J. Air Waste Manage., 55, 1527–1542, 2005.

Edgerton, E. S., Hartsell, B. E., Saylor, R. D., Jansen, J. J., Hansen, D. A., and Hidy, G. M.: The Southeastern Aerosol Research and Characterization Study, Part 3: Continuous measurements of fine particulate matter mass and composition, J. Air Waste Manage., 56, 1325–1341, 2006.

Fang, T., Verma, V., Guo, H., King, L. E., Edgerton, E. S., and Weber, R. J.: A semi-automated system for quantifying the oxidative potential of ambient particles in aqueous extracts using the dithiothreitol (DTT) assay: results from the Southeastern Center for Air Pollution and Epidemiology (SCAPE), Atmos. Meas. Tech. Discuss., 7, 7245–7279, doi:10.5194/amtd-7-7245-2014, 2014.

Gauderman, W. J., Vora, H., McConnell, R., Berhane, K., Gilliland, F., Thomas, D., Lurmann, F., Avoli, E., Kunzli, N., Jerrett, M., and Peters, J.: Effect of exposure to traffic on lung development from 10 to 18 years of age: a cohort study, Lancet, 369, 571–577, 2007.

Godri, K. J., Harrison, R. M., Evans, T., Baker, T., Dunster, C., Mudway, I. S., and Kelly, F. J.: Increased Oxidative Burden Associated with Traffic Component of Ambient Particulate Matter at Roadside and Urban Background Schools Sites in London, PLOS ONE, 6, doi:10.1371/journal.pone.0021961, 2011.

Hansen, D. A., Edgerton, E. S., Hartsell, B. E., Jansen, J. J., Kandasamy, N., Hidy, G. M., and Blanchard, C. L.: The southeastern aerosol research and characterization study: Part 1 – Overview, J. Air Waste Manage., 53, 1460–1471, 2003.

Hansen, D. A., Edgerton, E., Hartsell, B., Jansen, J., Burge, H., Koutrakis, P., Rogers, C., Suh, H., Chow, J., Zielinska, B., McMurry, P., Mulholland, J., Russell, A., and Rasmussen, R.: Air quality measurements for the aerosol research and inhalation epidemiology study, J. Air Waste Manage., 56, 1445–1458, 2006.

Harrison, R. M., Beddows, D. C. S., Hu, L., and Yin, J.: Comparison of methods for evaluation of wood smoke and estimation

of UK ambient concentrations, Atmos. Chem. Phys., 12, 8271–8283, doi:10.5194/acp-12-8271-2012, 2012.

Hecobian, A., Zhang, X., Zheng, M., Frank, N., Edgerton, E. S., and Weber, R. J.: Water-Soluble Organic Aerosol material and the light-absorption characteristics of aqueous extracts measured over the Southeastern United States, Atmos. Chem. Phys., 10, 5965–5977, doi:10.5194/acp-10-5965-2010, 2010.

Henshaw, J. M., Heithmar, E. M., and Hinners, T. A.: Inductively coupled plasma mass-spectrometric determination of trace-elements in surface waters subject to acidic deposition, Anal. Chem., 61, 335–342, doi:10.1021/Ac00179a011, 1989.

Hoek, G., Brunekreef, B., Goldbohm, S., Fischer, P., and van den Brandt, P. A.: Association between mortality and indicators of traffic-related air pollution in the Netherlands: a cohort study, Lancet, 360, 1203–1209, 2002.

Hu, S., Polidori, A., Arhami, M., Shafer, M. M., Schauer, J. J., Cho, A., and Sioutas, C.: Redox activity and chemical speciation of size fractioned PM in the communities of the Los Angeles-Long Beach harbor, Atmos. Chem. Phys., 8, 6439–6451, doi:10.5194/acp-8-6439-2008, 2008.

Kuenzli, N., Shi, T. M., Goetschi, T., Kelly, F., Mudway, I., Burney, P., Forsberg, B., Heinrich, J., Jarvis, D., Soon, A., Luczynska, C., Payo-Losa, F., Poli, A., Weyler, J., Hazenkamp, M., Norback, D., and Borm, P.: Beyond the mass: oxidative properties of PM$_{2.5}$ in the European Community Respiratory Health Survey (ECRHS), Epidemiology, 15, S43–S43, 2004.

Kumagai, Y., Arimoto, T., Shinyashiki, M., Shimojo, N., Nakai, Y., Yoshikawa, T., and Sagai, M.: Generation of reactive oxygen species during interaction of diesel exhaust particle components with NADPH-cytochrome P450 reductase and involvement of the bioactivation in the DNA damage, Free Radical Bio. Med., 22, 479–487, 1997.

Kumagai, Y., Koide, S., Taguchi, K., Endo, A., Nakai, Y., Yoshikawa, T., and Shimojo, N.: Oxidation of proximal protein sulfhydryls by phenanthraquinone, a component of diesel exhaust particles, Chem. Res. Toxicol., 15, 483–489, 2002.

Landreman, A. P., Shafer, M. M., Hemming, J. C., Hannigan, M. P., and Schauer, J. J.: A macrophage-based method for the assessment of the reactive oxygen species (ROS) activity of atmospheric particulate matter (PM) and application to routine (daily-24 h) aerosol monitoring studies, Aerosol Sci. Tech., 42, 946–957, 2008.

Li, N., Sioutas, C., Cho, A., Schmitz, D., Misra, C., Sempf, J., Wang, M. Y., Oberley, T., Froines, J., and Nel, A.: Ultrafine particulate pollutants induce oxidative stress and mitochondrial damage, Environ. Health Persp., 111, 455–460, 2003.

Li, N., Wang, M. Y., Bramble, L. A., Schmitz, D. A., Schauer, J. J., Sioutas, C., Harkema, J. R., and Nel, A. E.: The adjuvant effect of ambient particulate matter is closely reflected by the particulate oxidant potential, Environ. Health Persp., 117, 1116–1123, doi:10.1289/Ehp.0800319, 2009a.

Li, Q. F., Wyatt, A., and Kamens, R. M.: Oxidant generation and toxicity enhancement of aged-diesel exhaust, Atmos. Environ., 43, 1037–1042, doi:10.1016/j.atmosenv.2008.11.018, 2009b.

Lin, P. and Yu, J. Z.: Generation of reactive oxygen species mediated by humic-like substances in atmospheric aerosols, Environ. Sci. Technol., 45, 10362–10368, doi:10.1021/Es2028229, 2011.

Liu, Z. G., Berg, D. R., Swor, T. A., and Schauer, J. J.: Comparative analysis on the effects of diesel particulate filter and se-

lective catalytic reduction systems on a wide spectrum of chemical species emissions, Environ. Sci. Technol., 42, 6080–6085, doi:10.1021/Es8004046, 2008.

Marmur, A., Unal, A., Mulholland, J. A., and Russell, A. G.: Optimization-based source apportionment of PM$_{2.5}$ incorporating gas-to-particle ratios, Environ. Sci. Technol., 39, 3245–3254, doi:10.1021/Es0490121, 2005.

McWhinney, R. D., Zhou, S., and Abbatt, J. P. D.: Naphthalene SOA: redox activity and naphthoquinone gas–particle partitioning, Atmos. Chem. Phys., 13, 9731–9744, doi:10.5194/acp-13-9731-2013, 2013.

Mudway, I. S., Stenfors, N., Duggan, S. T., Roxborough, H., Zielinski, H., Marklund, S. L., Blomberg, A., Frew, A. J., Sandstrom, T., and Kelly, F. J.: An in vitro and in vivo investigation of the effects of diesel exhaust on human airway lining fluid antioxidants, Arch. Biochem. Biophys., 423, 200–212, doi:10.1016/j.abb.2003.12.018, 2004.

Norris, G. and Vedantham, R.: EPA Positive Matrix Factorization (PMF) 3.0 Fundamentals & User Guide, National Exposure Research Laboratory, US Environmental Protection Agency, Research Triangle Park, NC 27711, 2008.

Ntziachristos, L., Froines, J. R., Cho, A. K., and Sioutas, C.: Relationship between redox activity and chemical speciation of size-fractionated particulate matter, Part. Fibre Toxicol., 4, doi:10.1186/1743-8977-4-5, 2007.

Paatero, P.: Least squares formulation of robust non-negative factor analysis, Chemometr. Intell. Lab., 37, 23–35, doi:10.1016/S0169-7439(96)00044-5, 1997.

Peters, A., Veronesi, B., Calderón-Garcidueñas, L., Gehr, P., Chen, L. C., Geiser, M., Reed, W., Rothen-Rutishauser, B., Schürch, S., and Schulz, H.: Translocation and potential neurological effects of fine and ultrafine particles a critical update, Part. Fibre Toxicol., 3, doi:10.1186/1743-8977-3-13, 2006.

Riediker, M., Cascio, W. E., Griggs, T. R., Herbst, M. C., Bromberg, P. A., Neas, L., Williams, R. W., and Devlin, R. B.: Particulate matter exposure in cars is associated with cardiovascular effects in healthy young men, Am. J. Resp. Crit. Care, 169, 934–940, 2004.

Rodrigueza, C. E., Fukutoa, J. M., Taguchic, K., Froines, J., and Cho, A. K.: The interactions of 9,10-phenanthrenequinone with glyceraldehyde-3-phosphate dehydrogenase (GAPDH), a potential site for toxic actions, Chem.-Biol. Interact., 155, 97–110, 2005.

Saffari, A., Daher, N., Shafer, M. M., Schauer, J. J., and Sioutas, C.: Seasonal and spatial variation in dithiothreitol (DTT) activity of quasi-ultrafine particles in the Los Angeles Basin and its association with chemical species, J. Environ. Sci. Heal. A, 49, 441–451, doi:10.1080/10934529.2014.854677, 2014.

Sagai, M., Saito, H., Ichinose, T., Kodama, M., and Mori, Y.: Biological effects of diesel exhaust particles. 1. Invitro production of superoxide and invivo toxicity in mouse, Free Radical Bio. Med., 14, 37–47, 1993.

Samet, J. M., Dominici, F., Curriero, F. C., Coursac, I., and Zeger, S. L.: Fine particulate air pollution and mortality in 20 US cities, 1987–1994, New Engl. J. Med., 343, 1742–1749, 2000.

Sarnat, J. A., Marmur, A., Klein, M., Kim, E., Russell, A. G., Sarnat, S. E., Mulholland, J. A., Hopke, P. K., and Tolbert, P. E.: Fine particle sources and cardiorespiratory morbidity: an application of chemical mass balance and factor analytical source-

apportionment methods, Environ. Health Persp., 116, 459–466, doi:10.1289/Ehp.10873, 2008.

Schauer, J. J.: Evaluation of elemental carbon as a marker for diesel particulate matter, J. Expo. Anal. Env. Epid., 13, 443–453, 2003.

Schoonen, M. A. A., Cohn, C. A., Roemer, E., Laffers, R., Simon, S. R., and O'Riordan, T.: Mineral-induced formation of reactive oxygen species, Med. Mineral. Geochem., 64, 179–221, 2006.

Shi, T. M., Schins, R. P. F., Knaapen, A. M., Kuhlbusch, T., Pitz, M., Heinrich, J., and Borm, P. J. A.: Hydroxyl radical generation by electron paramagnetic resonance as a new method to monitor ambient particulate matter composition, J. Environ. Monitor., 5, 550–556, doi:10.1039/B303928p, 2003.

Stayner, L., Dankovic, D., Smith, R., and Steenland, K.: Predicted lung cancer risk among miners exposed to diesel exhaust particles, Am. J. Ind. Med., 34, 207–219, 1998.

Strickland, M. J., Darrow, L. A., Klein, M., Flanders, W. D., Sarnat, J. A., Waller, L. A., Sarnat, S. E., Mulholland, J. A., and Tolbert, P. E.: Short-term associations between ambient air pollutants and pediatric asthma emergency department visits, Am. J. Resp. Crit. Care, 182, 307–316, doi:10.1164/rccm.200908-1201OC, 2010.

Sun, J. D., Wolff, R. K., Kanapilly, G. M., and Mcclellan, R. O.: Lung retention and metabolic-fate of inhaled benzo(a)pyrene associated with diesel exhaust particles, Toxicol. Appl Pharmacol., 73, 48–59, 1984.

Talbot, J. and Weiss, A.: Laboratory methods for ICP-MS analysis of trace metals in precipitation, Hazardous Materials Lab, Hazardous Waste Research and Information Center, East Hazelwood, Champaign, IL 61820, 1994.

Tao, F., Gonzalez-Flecha, B., and Kobzik, L.: Reactive oxygen species in pulmonary inflammation by ambient particulates, Free Radical Bio. Med., 35, 327–340, doi:10.1016/S0891-5849(03)00280-6, 2003.

Venkatachari, P. and Hopke, P. K.: Development and laboratory testing of an automated monitor for the measurement of atmospheric particle-bound reactive oxygen species (ROS), Aerosol Sci. Tech., 42, 629–635, doi:10.1080/02786820802227345, 2008.

Verma, V., Ning, Z., Cho, A. K., Schauer, J. J., Shafer, M. M., and Sioutas, C.: Redox activity of urban quasi-ultrafine particles from primary and secondary sources, Atmos. Environ., 43, 6360–6368, 2009a.

Verma, V., Polidori, A., Schauer, J. J., Shafer, M. M., Cassee, F. R., and Sioutas, C.: Physicochemical and toxicological profiles of particulate matter in Los Angeles during the october 2007 southern California wildfires, Environ. Sci. Technol., 43, 954–960, 2009b.

Verma, V., Pakbin, P., Cheung, K. L., Cho, A. K., Schauer, J. J., Shafer, M. M., Kleinman, M. T., and Sioutas, C.: Physicochemical and oxidative characteristics of semi-volatile components of quasi-ultrafine particles in an urban atmosphere, Atmos. Environ., 45, 1025–1033, doi:10.1016/j.atmosenv.2010.10.044, 2011.

Verma, V., Rico-Martinez, R., Kotra, N., King, L., Liu, J., Snell, T. W., and Weber, R. J.: Contribution of water-soluble and insoluble components and their hydrophobic/hydrophilic subfractions to the reactive oxygen species-generating potential of fine ambient aerosols, Environ. Sci. Technol., 46, 11384–11392, 2012.

Warner, K. S., Eatough, D. J., and Stockburger, L.: Determination of fine particulate semi-volatile organic material at three eastern US sampling sites, J. Air Waste Manage., 51, 1302–1308, 2001.

Weber, R. J., Sullivan, A. P., Peltier, R. E., Russell, A., Yan, B., Zheng, M., de Gouw, J., Warneke, C., Brock, C., Holloway, J. S., Atlas, E. L., and Edgerton, E.: A study of secondary organic aerosol formation in the anthropogenic-influenced southeastern United States, J. Geophys. Res.-Atmos., 112, D13302, doi:10.1029/2007jd008408, 2007.

Wilson, D. W., Aung, H. H., Lame, M. W., Plummer, L., Pinkerton, K. E., Ham, W., Kleeman, M., Norris, J. W., and Tablin, F.: Exposure of mice to concentrated ambient particulate matter results in platelet and systemic cytokine activation, Inhal. Toxicol., 22, 267–276, doi:10.3109/08958370903278069, 2010.

Yan, B., Zheng, M., Hu, Y. T., Ding, X., Sullivan, A. P., Weber, R. J., Baek, J., Edgerton, E. S., and Russell, A. G.: Roadside, urban, and rural comparison of primary and secondary organic molecular markers in ambient PM$_{2.5}$, Environ. Sci. Technol., 43, 4287–4293, doi:10.1021/Es900316g, 2009.

Yang, A., Jedynska, A., Hellack, B., Rooter, I., Hoek, G., Brunekreef, B., Kuhlbusch, T. A. J., Cassee, F. R., and Janssen, N. A. H.: Measurement of the oxidative potential of PM$_{2.5}$ and its constituents: the effect of extraction solvent and filter type, Atmos. Environ., 83, 35–42, doi:10.1016/j.atmosenv.2013.10.049, 2014.

Zhang, X., Hecobian, A., Zheng, M., Frank, N. H., and Weber, R. J.: Biomass burning impact on PM$_{2.5}$ over the southeastern US during 2007: integrating chemically speciated FRM filter measurements, MODIS fire counts and PMF analysis, Atmos. Chem. Phys., 10, 6839–6853, doi:10.5194/acp-10-6839-2010, 2010.

Zhang, X., Liu, Z., Hecobian, A., Zheng, M., Frank, N. H., Edgerton, E. S., and Weber, R. J.: Spatial and seasonal variations of fine particle water-soluble organic carbon (WSOC) over the southeastern United States: implications for secondary organic aerosol formation, Atmos. Chem. Phys., 12, 6593–6607, doi:10.5194/acp-12-6593-2012, 2012.

Zhang, X. L., Lin, Y. H., Surratt, J. D., Zotter, P., Prevot, A. S. H., and Weber, R. J.: Light-absorbing soluble organic aerosol in Los Angeles and Atlanta: a contrast in secondary organic aerosol, Geophys. Res. Lett., 38, L21810, doi:10.1029/2011gl049385, 2011.